Application of Deep Neural Network in Estimation of the Weld Bead Parameters

Soheil Keshmiri, Xin Zheng, Chee Meng Chew, Chee Khiang Pang

***Abstract*— We present a deep learning approach to estimation of the bead parameters in welding tasks. Our model is based on a four-hidden-layer neural network architecture. More specifically, the first three hidden layers of this architecture utilize Sigmoid function to produce their respective intermediate outputs. On the other hand, the last hidden layer uses a linear transformation to generate the final output of this architecture. This transforms our deep network architecture from a classifier to a non-linear regression model. We compare the performance of our deep network with a selected number of results in the literature to show a considerable improvement in reducing the errors in estimation of these values. Furthermore, we show its scalability on estimating the weld bead parameters with same level of accuracy on combination of datasets that pertain to different welding techniques. This is a nontrivial result that is counter-intuitive to the general belief in this field of research.**

I. INTRODUCTION

The automation of the welding processes witness a significant advancement in recent decades. This, in turn, introduces a dramatic improvement on the manufacturing productivity and its efficiency. As the interest in automation of this field of industry continues to grow, the needs for quality research on reducing the manual modification of its parameters by human operator becomes indispensable. The intelligent monitoring of the welding process helps increase the precision and accuracy of the various aspects of its final outcome (e.g., the geometry of the weld beads). Furthermore, it helps determine if the driving parameters of the welding system requires readjustment. As a result, the overall performance of the system and consequently its welding quality improves significantly.

[6] uses the term Direct Weld Parameters (DWP) to refer to the geometrical description of the welding pool. The depth of penetration, the width of the weld bead, and the transverse cross-sectional areas are some of the examples of DWPs. Moreover, [1] shows the quality of these parameters are directly influenced by the control of the Indirect Weld Parameters (IWP). They include the voltage, the current, the torch traveling speed, the wire feed rate, and the arc gap. An investigation of the relationship between DWP and IWP is found in [20].

The study of the welding process and its related parameters can be broadly divided into two main fields of research. These are the estimation of the values of the weld parameters and the sensitivity analysis of these parameters. The sensitivity analysis refers to the prediction of the effect of the changes in welding process parameters on the final welding quality. It is applied on a number of welding techniques such as Gas Metal Arc Welding (GMAW) [10], Sub-merged Arc Welding (SAW) [12], [25], [22], and Tungsten Insert Gas (TIG) Welding [23]. On the other hand, the estimation problem attempts to predict these parameters, given the IWPs. In this article, we focus on the problem of the estimation of the welding process parameters.

There exists a rich body of research on estimation of the weld process parameters and its final outcome. [4] represents an early trial of static model, based on the heat flow. More specifically, it expresses the welding contour as a function of electrode velocity, heat input, and the material properties. Moreover, many researchers apply sophisticated mathematical models to capture this relationship. This includes factorial design [18], [9], [16], linear regression [24], [10], multiple regression analysis [19], response surface methodology [17], [8], Taguchi method [13], [15], or a combination of genetic algorithm and artificial neural network [27].

In particular, the recent achievements in application of artificial neural network (ANN) on modeling the welding process brings a remarkable progress in this area. They are successfully utilized to investigate the modeling of the welding process, the process control, and the estimation of the quality of the weld beads [7]. [26] uses ANN to model the arc welding process. This model achieves satisfactory results on the prediction accuracy of the weld bead parameters as compared to the conventional control systems. [21] uses back-propagation and counter-propagation to analyze the relationship between the input process parameters and the geometry of the weld bead in TIG welding. [3] studies the application of the self-organizing map (SOM) in monitoring and quality evaluation of the GMAW welding. [5] applies back-propagation on modeling and estimation of the weld bead parameters in Shielded Metal Arc Welding (SMAW).

In this article, we present a deep learning approach to estimation of the bead parameters in welding tasks. The deep networks learn through realization of the feature hierarchies with features from higher levels formed by the composition of those at the lower levels [28]. They are successfully used in a variety of applications ranging from natural language processing [29] to document recognition [31] and traffic sign classification [30]. An overview of the application of the deep network along with the challenges on training these architectures are found in [32] and [28], respectively.

This research is supported by the Keppel Corporation Ltd. under the project title *Productivity Enhancement of Yard Operation*, WBS:R-261-507-019-281

Soheil Keshmiri, Xin Zheng, Chee Meng Chew, Chee Khiang Pang are with Department of Mechanical Engineering, National University of Singapore {mpesohe, mpezhxi, mpeccm, justinpang}@nus.edu.sg

The scarcity of real welding data makes the analysis of the performance of proposed approaches difficult. The process of collecting such data is cumbersome and time-consuming. It requires hours of tedious welding by skilled welders. This is followed by long hours of manual measurement and cross sectional cutting to ascertain the weld bead parameters on a given workpiece. Moreover, there are a number of different welding techniques (e.g., arc and submerge arc weldings) whose applications are only appropriate for a certain type of welding tasks.

We compare the performance of our deep neural network architecture with a number of selected studies in the literature. In particular, we choose [26], [27], [22] for this purpose. These selected articles form a reliable representatives of the trends of the study in this field over the past two and half decades. More specifically, [26] is the seminal paper that first introduces the application of the single hidden layer neural network in estimation of the weld bead parameters. Furthermore, [22] applies a curvilinear approach to estimation of these parameters. Moreover, [27] proposes a single hidden layer neural network in combination with genetic algorithm to predict the weld bead parameters.

Additionally, the welding data of these studies are publicly available through their respective articles. They pertain to three different welding techniques. More specifically, [26] provides a dataset of size 42 on arc welding process. A dataset of size 28 is presented in [22]. It corresponds to submerged arc welding technique. The two tables that are included in [27] pertain to A-TIG welding process. These are comparably large datasets with 120 data each. Furthermore, they correspond to the application of A-TIG welding on two different types of materials. These are 304LN stainless steel and 316LN stainless steel.

Our contributions are as follows. First, we introduce the potentials that the deep neural networks can offer to the solution concept of the estimation of the weld bead parameters. To the best of our knowledge, this is the first attempt to apply deep neural computation in this field of research. Second, we show that its simple implementation achieves a considerable improvement over the results that are presented in the literature. In addition, its results do not require any additional post optimization processing as it is suggested by some of the reports in this field [27]. However, we acknowledge the fact that our approach is not the definite solution but an early step towards potentials that deep neural network can provide to estimation and analysis of the weld bead parameters. We are hopeful that it provides the researchers in automation of the welding processes with an opportunity to broaden their consideration on existing methodologies to advance the reliability of the performance of these systems.

The remainder of this article is organized as follows. Section II elaborates on formulation of our deep neural network architecture. We present the results of our case studies on a selected list of literature in section III. Section IV presents conclusion and future direction of this research.

II. Neural Architecture

We model our neural architecture as a four-hidden-layer deep network. We assign an equal number of neurons to each of these layers. In this architecture, the neurons of every preceding layer are fully connected to those of the succeeding layer via their corresponding weight matrices. Fig. 1 depicts this network. In this figure, we omit the neural units of the layers for simplicity. The inputs to this network are the welding process parameters. These are the current, the voltage, and the torch speed.

The first three hidden layers of this architecture utilize Sigmoid function to produce their respective intermediate outputs. As a result, the output values of these layers are bounded within $[0,1]$ interval. Whereas, the last hidden layer uses a linear transformation to generate the final output of this architecture. This transforms our deep network model from a classifier to a non-linear regression model. In other words, our architecture produces real-valued numbers to estimate the actual weld bead parameters. These outputs pertain to the depth of penetration and the width of the weld beads, respectively.

We train our deep network using feed-forward with back-propagation procedure. In addition, we use a constant momentum factor in calculation of the gradient of the weight matrices. This encourages their downhill movement during their updates. Furthermore, we formulate a linear cost function that utilizes the output of this network to minimize its discrepancy with the actual weld bead parameters in training data. Additionally, we regularize this cost function with the weighted sum of the weight matrices of every layer to prevent its over-fitting.

Let X denote the set of input parameters to the network. Furthermore, let Y be the set of weld bead parameters in training data. In addition, let $H^{(i)},\ i = 1,\ldots,4$, represent the i^{th} hidden layer of this architecture. Moreover, let $\Theta^{(i)}, i = 1,\ldots,5$, be the weight matrices that connect every preceding layer to its successor. This includes the connection between the input layer X to $H^{(1)}$ and the hidden layer $H^{(4)}$ to the output layer Y. There are three steps involved in formulation of our deep neural network. These are minimization of the cost function, feed-forward computation, and weight updates through back-propagation. We explain these steps in the following subsections.

A. Cost Function

During the training process, we are interested in weight matrices that minimize the discrepancy between the estimated values of the weld bead parameters by this neural

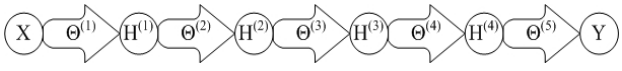

Fig. 1. Four-hidden-layer deep network architecture. X and Y are the input and the output layers of this architecture. $H^{(i)},\ i = 1\ldots4$ refers to the i^{th} hidden layer. $\Theta^{(i)},\ i = 1\ldots5$ are the weight matrices that connect the neurons of the i^{th} layer (including the input) to those at layer $i+1$. The neural units of these layers are omitted for simplicity.

architecture in contrast to their actual values in training data. Moreover, it is important to prevent the training process from overfitting on the training data. This increases the accuracy of the network in predicting the new weld bead parameters that do not come from the training set. Furthermore, this cost function needs to take into account the real-valued output of the last layer of our architecture. Therefore, we formulate our cost function as a regularized sum of the squared error of the output of the network and the actual bead parameters in the training data:

$$J = \frac{1}{2m}[(Y - Y')^2 + \lambda \sum_{l=1}^{L-1} \sum_{i=1}^{p^{(l)}} \sum_{j=1}^{q^{(l)}} (\Theta_{ji}^{(l)})^2] \tag{1}$$

where Y' is the estimated values of the weld bead parameters that are calculated by our neural architecture. m is the total number of training data. The second term in (1) is the regularization term that incorporates the sum of the squared of the weight matrices of all the layers in the network. This helps prevent the network from overfitting on the training data. λ is the regularization constant. L, $p^{(l)}$, and $q^{(l)}$ refer to the total number of hidden layers along with the row and the column dimensions of the weight matrix at l^{th} layer, respectively.

B. Feed-Forward

The values that are generated at every hidden layers are:

$$z^{(i)} = (H^{(i-1)})^T \times \Theta^{(i)} \tag{2}$$

$$H^{(i)} = \frac{1}{1 + e^{-z^{(i)}}},\ i = 1, \ldots, 4 \tag{3}$$

with $H^{(0)} = X$ in (2). These values correspond to the application of the Sigmoid transformation on the input as we move forward through layers of the network and towards the output layer. It is worth noting that we add an extra column with all whose entries equals to 1 to the input and the hidden layers to count for the bias term. This is why we do not explicitly include this term in (2). This also explains the starting indices of the last two summation operations from 1 in (1). The final output of this network is the linear transformation of the values at the last hidden layer i.e., $H^{(4)}$:

$$Y' = (H^{(4)})^T \times \Theta^{(5)} \tag{4}$$

where $\Theta^{(5)}$ is the weight matrix that transforms the values at the last hidden layer onto the final estimates of the bead parameters.

C. Back-Propagation and Weights Update

Equation (4) shows the final estimates of the values of the weld bead parameters by our neural architecture. The discrepancy between this generated output and the actual weld bead parameters in training data is:

$$\delta^{(Y)} = Y - Y' \tag{5}$$

We use this value to update $\Theta^{(5)}$:

$$\Delta^{(5)} = ((\delta^{(Y)})^T \times H^{(4)}) \times \gamma \tag{6}$$

$$\Theta^{(5)} = \Theta^{(5)} + \frac{1}{m}(\alpha \times \Delta^{(5)} + \lambda \sum_{i=1}^{p^{(5)}} \sum_{j=1}^{q^{(5)}} \Theta_{ji}^{(5)}) \tag{7}$$

where m is the total number of training data. $p^{(5)}$ and $q^{(5)}$ refer to the dimensions of the weight matrix of the output layer, as shown in Fig. 1. Equation (6) is the gradient of the output layer and γ is a constant that acts as the momentum to encourage the downhill move of the gradient values. We use $\gamma = 0.9$ throughout our experiments. Furthermore, α and λ are the learning rate and the regularization factor, respectively. Similarly, the updates of the weight matrices $\Theta^{(4)}$, $\Theta^{(3)}$, and $\Theta^{(2)}$ are:

$$\delta^{(i)} = (\Theta^{(i)})^T \times \delta^{(i+1)} \times (H^{(i)} \times (1 - H^{(i)})),\ i = 5, \ldots, 3 \tag{8}$$

$$\Delta^{(i-1)} = ((\delta^{(i)})^T \times H^{(i-1)}) \times \gamma \tag{9}$$

$$\Theta^{(i-1)} = \Theta^{(i-1)} + \frac{1}{m}(\alpha \times \Delta^{(i-1)} + \lambda \sum_{i=1}^{p^{(i-1)}} \sum_{j=1}^{q^{(i-1)}} \Theta_{ji}^{(i-1)}) \tag{10}$$

where $(H^{(i)} \times (1 - H^{(i)}))$ in (8) is the gradient of the Sigmoid function at the i^{th} hidden layer. The weight update for $\Theta^{(1)}$ closely follows (8) through (10) except that $H^{(i-1)}$ is replaced by X in (9):

$$\delta^{(2)} = (\Theta^{(2)})^T \times \delta^{(3)} \times (H^{(2)} \times (1 - H^{(2)})) \tag{11}$$

$$\Delta^{(1)} = ((\delta^{(2)})^T \times X) \times \gamma \tag{12}$$

$$\Theta^{(1)} = \Theta^{(1)} + \frac{1}{m}(\alpha \times \Delta^{(1)} + \lambda \sum_{i=1}^{p^{(1)}} \sum_{j=1}^{q^{(1)}} \Theta_{ji}^{(1)}) \tag{13}$$

The training process starts with the feed-forward calculation of the estimated output of the network. This is followed by the updates of the weight matrices through the back-propagation. Next, we calculate the cost function using the recently calculated output of the network and the updated weight matrices. This procedure continues until a given number of iterations is met.

III. Case Study

We compare the performance of our deep neural network architecture against a number of selected studies from the literature. In particular, we choose [26], [27], [22] for this purpose. These articles form a reliable representatives of the trends of research in this field over the past two and a half decades. More specifically, [26] is the seminal paper that first introduces the application of the single hidden layer neural network in estimation of the weld bead parameters. Furthermore, [22] applies a curvilinear approach to estimation of these parameters. Moreover, [27] proposes a single hidden layer neural network in combination with genetic algorithm to predict the weld bead parameters.

Additionally, the welding data of these studies are publicly available through their respective articles. These data pertain

to three main welding techniques. More specifically, [26] provides a dataset of size 42 on arc welding process. A dataset of size 28 is presented in [22]. It corresponds to submerged arc welding technique. The two tables that are included in [27] pertain to A-TIG welding process. These are comparably large datasets with 120 data each. Furthermore, they correspond to the application of A-TIG welding on 304LN stainless steel and 316LN stainless steel, respectively. Throughout our case study, we use the following abbreviations to refer to each of these datasets:

1) T_{1990}: dataset that is provided by [26] on arc welding process.
2) T_{2008}: dataset that is presented by [22] on submerge arc welding process.
3) $T_{2010}^{(1)}$ and $T_{2010}^{(2)}$: the two datasets in [27] on A-TIG welding on 304LN stainless steel and 316LN stainless steel, respectively.

A. Training Setup

We use 80% of data of each of these datasets for training purpose. We keep the remaining 20% for testing. These values are selected at random from each of these datasets. Moreover, we use the current, the voltage, and the torch speed as inputs to our neural architecture. These welding process parameters constitute the common features in [26], [22], [27] whose data are utilized throughout this case study. Similarly, we train our model on estimating the common weld bead parameters in these articles. They are the depth of penetration and the width of the weld beads, respectively. These choices of input and output parameters make the comparative analysis of the performance of our model in contrast to the above literature plausible. Furthermore, we compute two separate sets of weight matrices $\Theta^{(i)},\ i = 1,\ldots,5$. As a result, the weight matrices to estimate the depth of penetration and the width of the weld beads are different.

We train our model through a number of training phases with varying iterations. More specifically, we train this netwrok using 1000 through 6000 iterations where each setting of the number of iterations correspond to a different training phase. This is to choose the best meta-parameters that fit our architecture with respect to a given dataset. These parameters are the learning rate α, the regularization factor λ, and the number of neural units at every hidden layer of our network. However, we use a fixed momentum $\gamma = 0.9$ throughout these training phases. It is worth noting that we assign same number of neurons to all the hidden layers.

We initialize these meta-parameters from their respective predefined sets of values at the commencement of every training phase. For instance, we initialize λ to a value that is selected from $[0, 0.001, 0.003, 0.009, 0.01, 0.03, 0.09, 0.1, 0.3, 0.9, 1, 3, 10, 20, 30]$ and train the network in a given phase. The initialization of the value of a meta-parameter is carried out in a sequential order of its corresponding initialization set. Similarly, we use $[0, 0.001, 0.003, 0.009, 0.01, 0.03, 0.09, 0.1, 0.3, 0.9, 1, 3, 10, 20, 30, \ldots, 100]$ and $[2, \ldots, 10]$ to initialize the α and the number of neural units of the hidden layers, respectively. This process is performed through a series of nested loops in our implementation. We update these meta-parameters if the result of the estimate of the weld bead parameters in a training phase outperforms the previous result.

Table I shows the final values of these meta-parameters along with the best number of iterations for depth of penetration. Similarly, Table II corresponds to their values in estimating the width of weld bead. The last column of these tables shows the size of each of the corresponding dataset for comparison. These tables reveal the overall simplicity of our deep network architecture. More specifically, the number of neural units of each of the hidden layer of this network is between 2 to 5 neurons. This expedites its convergence since less computational units results in smaller weight matrices at each layer. Furthermore, its computation favors a setting where the regularization term is excluded. This is evident in the λ entry of these tables with whose values mostly zero. This suggests that our model does not suffer from over-fitting in general. The only exception to this observation is T_{2008} [22]. This is mainly due to the small size of this dataset (28 data in total) which can lead to over-fitting during a particular training phase.

Moreover, the maximum number of iterations to train this network does not exceed 4000. However, its variation does not exhibit any correspondence with the size of the given datasets. As a result, any conclusion on the effect of the size of the dataset on training process in these cases are not warranted. However, the learning rate α exhibits a comparably higher variations in these tables. This is indicative of high variance among the values of the depth of penetration and the width of the weld beads in training data.

TABLE I

BEST SET OF META-PARAMETERS TO ESTIMATE THE DEPTH OF PENETRATION IN A GIVEN DATASET.

Dataset	No. Neurons	α	λ	Iterations	Size
T_{1990}	5	50.0	0.0	4000	42
T_{2008}	4	10.0	0.09	1000	28
$T_{2010}^{(1)}$	5	10.0	0.0	2000	120
$T_{2010}^{(2)}$	3	40.0	0.0	4000	120

TABLE II

BEST SET OF META-PARAMETERS TO ESTIMATE WIDTH OF THE WELD BEAD IN A GIVEN DATASET.

Dataset	No. Neurons	α	λ	Iterations	Size
T_{1990}	5	50.0	0.0	4000	42
T_{2008}	4	10.0	0.3	3000	28
$T_{2010}^{(1)}$	2	30.0	0.0	1000	120
$T_{2010}^{(2)}$	4	10.0	0.0	4000	120

B. Results

Tables III through VI show the result of the performance of our deep network architecture on the test data in comparison with the single hidden layer net [26], the curvilinear model [22], and the combination of single hidden layer network and genetic algorithm [27]. The test data pertains to a 20% subset of entire values of each of these datasets that are selected at random. However, we are unable to use the exact same test data in these articles since the authors do not report these values. The row entry DNN of these tables are the results obtained by our deep neural network. We choose Root Mean Squared Error (RMS) and the percentage of Prediction Error (PE) to report our results. The main reason to choose these two values are to enable the comparative analysis of our results with respect to the selected literature. More specifically, [26] reports the percentage of prediction error. Whereas, [22] and [27] provide RMS as the measure of accuracy of their models.

A comparison between the PE in Table III reveals that the standard deviation of the differences between these values is above one standard deviation. As a result, the reduction of the percentage of the prediction error by our model on this dataset is significant. Additionally, the RMS values that are calculated by our model are considerably small on this dataset (in the scale of millimeter). However, we are unable to confirm the significance of these values since [26] does not provide any report on RMS values of their one-hidden-layer network.

We notice the same trend of improvement on the entries of Tables IV through VI. The PE values that are calculated by our model on these datasets are below 2.55%. Moreover, it considerably improves upon the RMS values in Table IV. It reduces these values to almost half their values in [22] as it is evident in the entries of this table. The same observation on reduction of the values of the RMS is valid in case of Tables V and VI. However, the latter improvements are within one standard deviation of the RMS reported in [27].

TABLE III

RMS AND PE RESULTS OF OUR DEEP NEURAL ARCHITECTURE IN COMPARISON TO TABLE T_{1990} ON TEST DATA.

	Penetration(mm)		Width	
	RMS	PE	RMS	PE
DNN	0.081	2.91%	0.115	1.08%
T_{1990}	—	19.58%	—	5.68%

TABLE IV

RMS AND PE RESULTS OF OUR DEEP NEURAL ARCHITECTURE IN COMPARISON TO TABLE T_{2008} ON TEST DATA.

	Penetration(mm)		Width	
	RMS	PE	RMS	PE
DNN	0.148	2.27%	0.150	1.21%
T_{2008}	0.292	—	0.353	—

TABLE V

RMS AND PE RESULTS OF OUR DEEP NEURAL ARCHITECTURE IN COMPARISON TO TABLE T^1_{2010} ON TEST DATA.

	Penetration(mm)		Width	
	RMS	PE	RMS	PE
DNN	0.091	2.28%	0.163	2.35%
$T^{(1)}_{2014}$	0.148	—	0.205	—

TABLE VI

RMS AND PE RESULTS OF OUR DEEP NEURAL ARCHITECTURE IN COMPARISON TO TABLE T^2_{2010} ON TEST DATA.

	Penetration(mm)		Width	
	RMS	PE	RMS	PE
DNN	0.108	2.01%	0.124	2.52%
$T^{(1)}_{2014}$	0.124	—	0.156	—

Hence, its statistical significance is not warranted.

An interesting observation on the results of the performance of our deep network architecture is its stability on estimating the weld bead parameters, irrespective of the dataset that is used. In particular, the differences between the RMS and the PE values that are generated by our model in Tables III through VI are within one standard deviation of one another. In other words, our deep neural architecture is capable of adjusting to different settings of input parameters to estimate the values of the output parameters within an acceptable range of accuracy.

C. Scalability on Combined Datasets

In this section, we analyze the performance of our model on combination of these datasets. In particular, we report the RMS and the PE values of our deep network on the following two datasets:

1) $T^{(1,2)}_{2010}$: is the combination of $T^{(1)}_{2010}$ and $T^{(2)}_{2010}$ in [27].
2) T_{all}: combines all these datasets into one.

We choose the same ratio of 80% train data and 20% test data on these two new datasets. The test data is selected at random after combining all the values in one large dataset. Tables VII and VIII show the best fit of meta-parameters for these datasets. An interesting observation to note is the increase in the number of neural units on combination of these datasets as compared to Tables I and II. Such an increase in the number of neural units in hidden layers is due to the increase of the size of the resultant combined datasets. The value of λ for estimating the width of the weld beads in Table VIII is also slightly higher than those in Tables I, II, and VII. It suggests that our model is more susceptible to over-fitting on estimating the width of the weld beads in this combined dataset. However, the learning rate α remains in the same range as in Tables I and II.

Table IX provides the RMS and the PE values that are calculated by our deep network on these combined datasets.

TABLE VII

BEST SET OF META-PARAMETERS TO ESTIMATE THE DEPTH OF PENETRATION ON COMBINATION OF DATASETS.

Dataset	No. Neural Units	α	λ	No. Iterations
$T_{2010}^{(1,2)}$	7	30	0.0	4000
T_{all}	9	10	0.001	4000

TABLE VIII

BEST SET OF META-PARAMETERS TO ESTIMATE WIDTH OF THE WELD BEAD ON COMBINATION OF DATASETS.

Dataset	No. Neural Units	α	λ	No. Iterations
$T_{2010}^{(1,2)}$	4	10	0.9	1000
T_{all}	7	30	0.0	2000

Although these values are slightly larger than those calculated on separate datasets by our model, their differences are within one standard deviation from one another. This is an interesting observation that challenges the general belief in this field of research. In particular, it shows that a deep neural network is capable of discovering the pattern that can exist among the weld bead parameters that pertain to different type of welding processes. However, this observation requires further investigation.

IV. CONCLUSIONS

In this article, we present a deep learning approach to estimation of the bead parameters in welding tasks. We show that the linear transformation of the output layer enables our deep network to behave as a non-linear regression model to generate real-valued estimate of the weld bead parameters. A comparison between our model and a selected number of results in the literature show a considerable improvement in reducing the errors in estimation of these values. Furthermore, we show its scalability on estimating these values with the same level of accuracy on combination of datasets of different welding techniques. This is a nontrivial result that is counter-intuitive to the general belief in this field of research.

The RMS entries of Tables III through IX reveal that the estimate of the depth of penetration always yields a better result as compared to that of the width of the weld beads. Moreover, this observation holds true in case of our deep network architecture as well as methodologies that are adapted by the selected literature in this case study. Furthermore, the same behavior is noticeable in the results obtained from the combined datasets. The future direction of this research pertains to analysis of this peculiar behavior to realize the possibility of further reduction of the errors on estimation of the width of the weld beads.

In this study, we apply our approach to the data that pertains to three different welding techniques. This is mainly due to scarcity of data on other welding techniques. We are hopeful to find data on other variety of welding techniques to realize the utility of our model on broader welding applications. Moreover, it is interesting to investigate the performance of our model on the results of the multi-pass welding processes once its data is available.

TABLE IX

RMS AND PE RESULTS OF OUR DEEP NEURAL ARCHITECTURE ON TEST DATA OF COMBINATION OF DATASETS.

	Penetration(mm)		Width	
	RMS	PE	RMS	PE
$T_{2010}^{(1,2)}$	0.165	3.90%	0.196	3.49%
T_{all}	0.197	4.02%	0.204	2.96%

ACKNOWLEDGMENT

The authors thank the National Research Foundation, Keppel Corporation and National University of Singapore for supporting this research that is carried out in the Keppel-NUS Corporate Laboratory (project title: *Productivity Enhancement of Yard Operation*, WBS:R-261-507-019-281). The conclusions put forward reflect the views of the authors alone, and not necessarily those of the institutions within the Corporate Laboratory.

REFERENCES

[1] A.C. Nunes, An extended Rosenthal weld model, Welding J., pp. 165-170, 1983

[2] K. Andersen, G. Cook, G. Karsai, and K. Ramaswamy, Artificial neural network applied to arc welding process modeling and control, IEEE J. Trans. Ind. Appl., vol. 26, no. 5, pp. 824-830, 1990

[3] C.S. Wu, T. Polte and D. Rehfeldt, Gas metal arc welding process monitoring and quality evaluation using neural network, Sci. Technol. Welding Joining, vol. 5, no. 5, pp. 324328, 2000

[4] D. Rosenthal, Mathematical theory of heat distribution during welding and cutting, Welding J., vol. 20, no. 5, pp. 220-234, 1941

[5] D.S. Nagesh, and G.L. Datta, Prediction of weld bead geometry and penetration in shielded metal-arc welding using artificial neural networks, J. Mater. Process. Technol., vol. 123, pp. 303312, 2002

[6] G. E. Cook, Feedback and adaptive control in automated arc welding systems, Metal Construction, vol. 13, no. 9, pp.551-556, 1981

[7] G.E. Cook, R.J. Barnett, K. Anderson, and A.M. Strauss, Weld modeling and control using artificial neural networks, IEEE Trans. Indus. Appl., vol. 31, no. 6, pp. 14841491, 1995

[8] N. Gunaraj, and V. Murugan, Prediction and control of weld bead geometry and shape relationships in submerged arc welding of pipes, J. Mater Process Technol, vol. 168, pp. 478-87, 2005

[9] V. K. Gupta and R. S. Parmar RS, Fractional factorial technique to predict dimensions of the weld bead in automatic submerged arc welding, IE (I) J-MC; vol. 70 (November), pp. 6775, 1989

[10] I.S. Kim, K.J. Son, Y.S. Yang, and P.K.D.V. Yaragada, Sensitivity analysis for process parameters in GMA welding processes using a factorial design method, Int. J. Mach. Tools Manuf., vol. 43, pp. 763-769, 2003

[11] J.J. Hunter, G.W. Bryce, and J. Doherty, On-line control of the arc welding process, in Int. Conf. Development in Mechanized Automated and Robotic Welding, International Conference, pp. 37.1-12, 1980

[12] J.E.R. Dhas and M. Satheesh, Sensitivity analysis of submerged arc welding parameters for low ally steel weldment, Indian J. of Eng. & Materials Sci, Vol. 20, pp. 425-434, 2013

[13] S. C. Juang and Y. S. Tarng, Process parameters selection for optimizing the weld pool geometry in the tungsten inert gas welding of stainless steel, J. Mater. Process Technol., pp. 122:33-7, 2002

[14] I. S. Kim, J. S. Son, I. G. Kim, and O. S. Kim, A study on relationship between process variable and bead penetration for robotic CO2 arc welding, J. Mater. Process Tech., vol. 136, pp. 139-45, 2003

[15] H. K. Lee, H. S. Han, K. J. Son, and S. B. Hong, Optimization of Nd-YAG laser welding parameters for sealing small titanium tube ends, J. Mater. Sci. Eng., A415, pp. 149-55, 2006

[16] N. Murugan and R. S. Parmar, Effects of MIG process parameters on the geometry of the bead in the automatic surfacing of stainless steel, J. Mater. Process Technol, vol. 41, pp. 381-98, 1994

[17] N. Murugan and R. S. Parmar, Effects of welding conditions on microstructure and properties of tupe 316L stainless steel submerged arc welding cladding, Weld J., vol. 76, no. 5, pp. 210-20, 1997

[18] J. Raveendra and R. S. Parmar, Mathematical models to predict weld bead geometry for ux cored arc welding, J. Metal Construct, vol. 19, no. 2, pp. 31R5R, 1987

[19] S. Rajakumar, C. Muralidharan, and V. Balasubramanian, Statistical analysis to predict grain size and hardness of the weld nugget of friction-stir-welded AA6061-T6 aluminum alloy joints, Int. J. of Advanced Manufacturing Technology, vol. 57, no. 1-4, pp. 151-165, 2011

[20] R.S. Chandel, S. Bala, Relationship between submerged arc welding parameters and weld bead size, Schweissen Schneiden, vol. 40, no. 2, pp. 28-31 (88-91), 1998

[21] S.C. Juang, Y.S. Tarng, and H.R. Lii, A comparison between the back propagation and counter-propagation networks in the modeling of the TIG welding process, J. Mater. Process. Technol., vol. 75, pp. 5462, 1998

[22] S. Karaoglu and A. Secgin, Sensitivity analysis of submerged arc welding process parameters, J. Mater. processing technology, vol. 202, pp. 500-507, 2008

[23] Y. L. Xu, , Z. B. Dong, Y. H. Wei, and C. L. Yang, Marangoni convection and weld shape variation in A-TIG welding process, Theoretical and applied fracture mechanics, vol. 48, no. 2, pp. 178-186, 2007

[24] L. J. Yang, M. J. Bibby, and R. S. Chandel, Linear regression equations for modeling the submerged-arc welding process, J. Mater. Process Technol, vol. 39, pp. 33-42, 1993

[25] Y.S. Tarng, W.H. Yang, S.C. Juang, The use of fuzzy logic in the Taguchi method for the optimization of the submerged arc welding process, Int. J. Adv. Manuf. Technol., vol. 16, pp. 688-694, 2000

[26] K. Anderson, G. Cook, G. Karsai, and K. Ramaswamy, artificial neural networks applied to arc welding process modeling and control, IEEE Trans. on Industry Applications, Vol. 26, no. 5, pp. 824-830, 1990

[27] N. ChandrasekharM. Vasudevan, Intelligent modeling for optimization of a A-TIG welding process, Mater. and Manufacturing Processes, vol. 25, pp. 1341-1350, 2010

[28] G. Xavier and Y. Bengio, Understanding the difficulty of training deep feedforward neural networks, in Int. Conf. Artificial Intelligence and Statistics, 2010.

[29] R. Collobert and J. Weston, A unified architecture for natural language processing: Deep neural networks with multitask learning, in Int. Conf. Machine Learning, 2008.

[30] D. C. Ciresan, U. Meier, J. Masci, and J. Schmidhuber, Multi-column deep neural network for traffic sign classification, Neural Networks, vol. 32, pp. 333-338, 2012.

[31] Y. LeCun, L. Bottou, and P. Haffiner Gradient-based learning applied document recognition, Proceedings of the IEEE, vol. 86, pp. 2278-2324, 1998.

[32] J. Masci, and J. Schmidhuber, Deep Learning in Neural Networks: An Overview, Neural Networks, vol. 61, pp. 85-117, 2015.